

Effect of Heme Modification on Oxygen Affinity of Myoglobin and Equilibrium of the Acid–Alkaline Transition in Metmyoglobin

Tomokazu Shibata,[†] Satoshi Nagao,^{†,‡} Masashi Fukaya,[†] Hulin Tai,[†]
Shigenori Nagatomo,[†] Kenji Morihashi,[†] Takashi Matsuo,[§] Shun Hirota,[§]
Akihiro Suzuki,[⊥] Kiyohiro Imai,[¶] and Yasuhiko Yamamoto^{*,†}

Department of Chemistry, University of Tsukuba, Tsukuba 305-8571, Japan, Graduate School of Materials Science, Nara Institute of Science and Technology, Nara 630-0192, Japan, Department of Materials Engineering, Nagaoka National College of Technology, Nagaoka 940-8532, Japan, and Department of Frontier Bioscience, Faculty of Bioscience and Applied Chemistry, Hosei University, Tokyo 184-8584, Japan

Received November 23, 2009; E-mail: yamamoto@chem.tsukuba.ac.jp

Abstract: Functional regulation of myoglobin (Mb) is thought to be achieved through the heme environment furnished by nearby amino acid residues, and subtle tuning of the intrinsic heme Fe reactivity. We have performed substitution of strongly electron-withdrawing perfluoromethyl (CF₃) group(s) as heme side chain(s) of Mb to obtain large alterations of the heme electronic structure in order to elucidate the relationship between the O₂ affinity of Mb and the electronic properties of heme peripheral side chains. We have utilized the equilibrium constant (pK_a) of the “acid–alkaline transition” in metmyoglobin in order to quantitatively assess the effects of the CF₃ substitutions for the electron density of heme Fe atom (ρ_{Fe}) of the protein. The pK_a value of the protein was found to decrease by ~1 pH unit upon the introduction of one CF₃ group, and the decrease in the pK_a value with decreasing the ρ_{Fe} value was confirmed by density functional theory calculations on some model compounds. The O₂ affinity of Mb was found to correlate well with the pK_a value in such a manner that the P₅₀ value, which is the partial pressure of O₂ required to achieve 50% oxygenation, increases by a factor of 2.7 with a decrease of 1 pK_a unit. Kinetic studies on the proteins revealed that the decrease in O₂ affinity upon the introduction of an electron-withdrawing CF₃ group is due to an increase in the O₂ dissociation rate. Since the introduction of a CF₃ group substitution is thought to prevent further Fe²⁺–O₂ bond polarization and hence formation of a putative Fe³⁺–O₂⁻-like species of the oxy form of the protein [Maxwell, J. C.; Volpe, J. A.; Barlow, C. H.; Caughey, W. S. *Biochem. Biophys. Res. Commun.* **1974**, *58*, 166–171], the O₂ dissociation is expected to be enhanced by the substitution of electron-withdrawing groups as heme side chains. We also found that, in sharp contrast to the case of the O₂ binding to the protein, the CO association and dissociation rates are essentially independent of the ρ_{Fe} value. As a result, the introduction of electron-withdrawing group(s) enhances the preferential binding of CO to the protein over that of O₂. These findings not only resolve the long-standing issue of the mechanism underlying the subtle tuning of the intrinsic heme Fe reactivity, but also provide new insights into the structure–function relationship of the protein.

Introduction

Myoglobin (Mb), an oxygen storage hemoprotein, has long served as a paradigm for the structure–function relationships of metalloproteins.^{1,2} Dioxygen (O₂) is reversibly bound to a ferrous heme Fe atom in Mb, and the O₂ affinity of the protein is generally represented by the P₅₀ value, which is the partial

pressure of O₂ required to achieve 50% oxygenation. The structural basis for the control of the O₂ affinity of Mb has been investigated exhaustively for many years.^{3–11} The regulation

[†] Department of Chemistry, University of Tsukuba.
[‡] Present address: Graduate School of Materials Science, Nara Institute of Science and Technology (NAIST), Nara 630-0192, Japan.
[§] Graduate School of Materials Science, Nara Institute of Science and Technology (NAIST).
[⊥] Department of Materials Engineering, Nagaoka National College of Technology.
[¶] Department of Frontier Bioscience, Faculty of Bioscience and Applied Chemistry, Hosei University.
(1) Chu, K.; Vojtechovsky, J.; McMahon, B. H.; Sweet, R. M.; Berendzen, J.; Schlichting, I. *Nature* **2000**, *403*, 921–923.

(2) Schotte, F.; Lim, M.; Jackson, T. A.; Smirnov, A. V.; Soman, J.; Olson, J. S.; Phillips, G. N., Jr.; Wulff, M.; Anfinrud, P. A. *Science* **2003**, *300*, 1944–1947.
(3) Antonini, E.; Brunori, M. In *Hemoglobins and Myoglobins and their Reactions with Ligands*; North Holland Publishing: Amsterdam, 1971; pp 43–48.
(4) Springer, B. A.; Sligar, S. G.; Olson, J. S.; Phillips, G. N., Jr. *Chem. Rev.* **1994**, *94*, 699–714.
(5) Olson, J. S.; Phillips, G. N., Jr. *J. Biol. Inorg. Chem.* **1997**, *2*, 544–552.
(6) Capece, L.; Marti, M. A.; Crespo, A.; Doctorovich, F.; Estrin, D. A. *J. Am. Chem. Soc.* **2006**, *128*, 12455–12461.
(7) Falk, J. E.; Phillips, J. N.; Magnusson, E. A. *Nature* **1966**, *212*, 1531–1533.
(8) Caughey, W. S. *Annu. Rev. Biochem.* **1967**, *36*, 611–644.

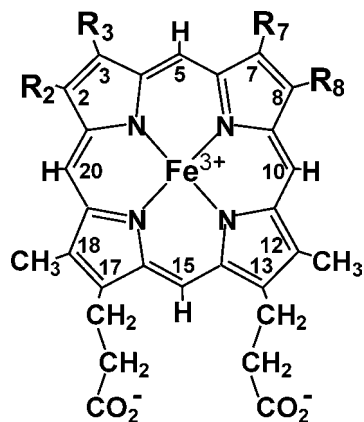
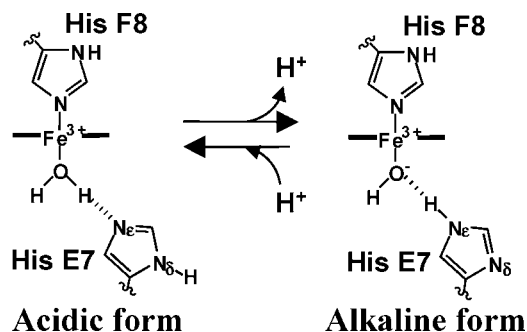


Figure 1. Structures and numbering system for protoheme ($R_2 = \text{CH}_3$, $R_3 = R_8 = \text{CH}=\text{CH}_2$, $R_7 = \text{CH}_3$), mesoheme ($R_2 = R_7 = \text{CH}_3$, $R_3 = R_8 = \text{C}_2\text{H}_5$), 7-PF ($R_2 = \text{CH}_3$, $R_3 = R_8 = \text{C}_2\text{H}_5$, $R_7 = \text{CF}_3$), 2,8-DPF ($R_2 = R_8 = \text{CF}_3$, $R_3 = R_7 = \text{CH}_3$), and deuteroheme ($R_2 = R_7 = \text{CH}_3$, $R_3 = R_8 = \text{H}$).

of the Mb function is thought to be achieved through the heme environment furnished by nearby amino acid residues, and subtle tuning of the intrinsic heme Fe reactivity. Although the heme environmental effects on the O_2 affinity of the protein have been elucidated in some detail,^{4–6} the relationship between the heme electronic structure and Fe reactivity has remained to be clarified. Although extensive heme modification studies have been performed to reveal the molecular mechanisms underlying the tuning of the Fe reactivity,^{9–13} the relationship between the properties of heme peripheral side chains and the O_2 affinity of Mb has been controversial.^{9–11} The difficulty in these studies was mainly two-fold; (1) the variation in the heme modification was not large enough to allow quantitative characterization of the structure–function relationship of Mb and (2) a lack of an appropriate parameter that quantitatively represents the effect of the heme modification on the properties of the heme Fe atom in the protein.

In this study, we have performed the substitution of strongly electron-withdrawing perfluoromethyl (CF_3) group(s), as heme side chain(s), for large and stepwise alterations of the heme electronic structure using the reported procedure.^{14,15} Mesoheme (Meso), 13,17-bis(2-carboxylatoethyl)-3,8-diethyl-2,12,18-trimethyl-7-trifluoromethylporphyrinato-iron(III)¹⁴ (7-PF), and 13,17-bis(2-carboxylatoethyl)-3,7-diethyl-12,18-trimethyl-2,8-ditrifluoromethylporphyrinato-iron(III) (2,8-DPF (see Supporting Information)) were incorporated into the apoprotein of Mb to prepare reconstituted Mbs, i.e., Mb(Meso), Mb(7-PF), and Mb(2,8-DPF), respectively. These hemes differ in the numbers of CF_3 , CH_3 , and C_2H_5 side chains (Figure 1). The use of these hemes affords large variation in the electronic structure of the

Scheme 1. Acid–alkaline Transition in metMb

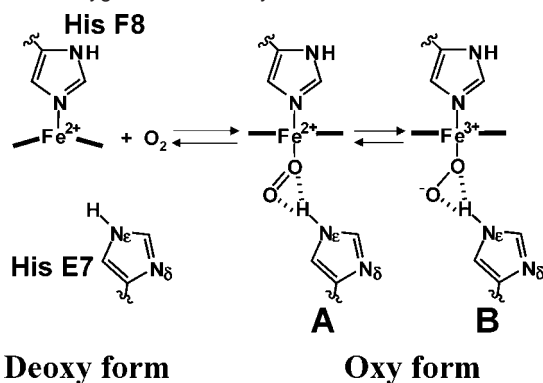


porphyrin moiety of the heme, which allows detailed characterization of the relationship between the properties of heme peripheral side chains and the O_2 affinity of Mb.

In order to quantitatively assess the effects of the CF_3 substitution(s) on the electron density of the heme Fe atom (ρ_{Fe}) in the protein, we used the equilibrium constant of the “acid–alkaline transition” in metmyoglobin (metMb),^{3,16–27} together with density functional theory (DFT) calculations. The heme active site of metMb exhibits characteristic pH-dependent structure changes collectively known as the acid–alkaline transition.³ The metMb possessing highly conserved distal His E7 (E7 represents an alphanumeric code referring to the positions of amino acid residues in the helices and turns of Mb, E7 representing the seventh residue in the E helix) has H_2O and OH^- as coordinated external ligands under low and high pH conditions, respectively.²⁸ As illustrated in Scheme 1, the acid–alkaline transition in the protein comprises three distinct reactions, i.e., interconversion of the coordinated ligand between H_2O and OH^- , tautomerism of the His E7 imidazole, and deprotonation/protonation of His E7 N_δH .²⁸ Furthermore, since the transition is associated with the deprotonation/protonation process, its equilibrium constant is usually represented as the pK_a value, and this value has been shown to be highly sensitive to the heme electronic structure of the protein.^{18,27} In addition, upon the transition from the acidic form to the alkaline one (Scheme 1), the Fe-bound ligand changes from H_2O to OH^- , with a concomitant change in the spin state from the ferric high

- (9) Sono, M.; Asakura, T. *J. Biol. Chem.* **1975**, *250*, 5227–5232.
 (10) Sono, M.; Smith, P. D.; McCray, J. A.; Asakura, T. *J. Biol. Chem.* **1976**, *251*, 1418–1426.
 (11) Kawabe, K.; Imaizumi, K.; Imai, K.; Tyuma, I.; Ogoshi, H.; Iwahara, T.; Yoshida, Z. *J. Biochem.* **1982**, *92*, 1703–1712.
 (12) Matsuo, T.; Dejima, H.; Hirota, S.; Murata, D.; Sato, H.; Ikegami, T.; Hori, H.; Hisaeda, Y.; Hayashi, T. *J. Am. Chem. Soc.* **2004**, *126*, 16007–16017; Hayashi, T.; Dejima, H.; Matsuo, T.; Sato, H.; Murata, D.; Hisaeda, Y. *J. Am. Chem. Soc.* **2002**, *124*, 11226–11227.
 (13) Neya, S.; Funasaki, N.; Shiro, Y.; Iizuka, T.; Imai, K. *Biochim. Biophys. Acta* **1994**, *1208*, 31–37.
 (14) Toi, H.; Homma, M.; Suzuki, A.; Ogoshi, H. *J. Chem. Soc., Chem. Commun.* **1985**, 1791–1792.
 (15) Ono, N.; Kawamura, H.; Maruyama, K. *Bull. Chem. Soc. Jpn.* **1986**, *62*, 3386–3388.

- (16) Giacometti, G. M.; Da Ros, A.; Antonini, E.; Brunori, M. *Biochemistry* **1975**, *14*, 1584–1588.
 (17) Iizuka, T.; Morishima, I. *Biochim. Biophys. Acta* **1975**, *400*, 143–153.
 (18) McGrath, T. M.; La Mar, G. N. *Biochim. Biophys. Acta* **1978**, *534*, 99–111.
 (19) Pande, U.; La Mar, G. N.; Lecomte, J. T. L.; Ascoli, F.; Brunori, M.; Smith, K. M.; Pandey, R. K.; Parish, D. W.; Thanabal, V. *Biochemistry* **1986**, *25*, 5638–5646.
 (20) Yamamoto, Y.; Osawa, A.; Inoue, Y.; Chūjō, R.; Suzuki, T. *Eur. J. Biochem.* **1990**, *192*, 225–229.
 (21) Yamamoto, Y.; Chūjō, R.; Inoue, Y.; Suzuki, T. *FEBS Lett.* **1992**, *310*, 71–74.
 (22) Yamamoto, Y.; Suzuki, T.; Hori, H. *Biochim. Biophys. Acta* **1993**, *1203*, 267–275.
 (23) Yamamoto, Y.; Hirai, Y.; Suzuki, A. *J. Biol. Inorg. Chem.* **2000**, *5*, 455–462.
 (24) Hirai, Y.; Yamamoto, Y.; Suzuki, A. *Bull. Chem. Soc. Jpn.* **2000**, *73*, 2309–2316.
 (25) Yamamoto, Y.; Nagao, S.; Hirai, Y.; Inose, T.; Terui, N.; Mita, H.; Suzuki, A. *J. Biol. Inorg. Chem.* **2004**, *9*, 152–160.
 (26) Hirai, Y.; Nagao, S.; Mita, H.; Suzuki, A.; Yamamoto, Y. *Bull. Chem. Soc. Jpn.* **2004**, *77*, 1485–1486.
 (27) Nagao, S.; Hirai, Y.; Suzuki, A.; Yamamoto, Y. *J. Am. Chem. Soc.* **2005**, *127*, 4146–4147.
 (28) Shu, F.; Ramakrishnan, V.; Schoenborn, B. P. *Proc. Natl. Acad. Sci. U.S.A.* **2000**, *97*, 3872–3877.

Scheme 2. Oxygenation of deoxy Mb^a

^a The binding of O₂ to the heme Fe is stabilized by the hydrogen-bonding between the Fe-bound O₂ and distal His (His E7).^{5,29} Structure (B) of the oxy form is only a proposed one.^{5,30,31}

spin (HS) one, i.e., $S = 5/2$, to the ferric low spin (LS) one, i.e., $S = 1/2$.³ Hence, despite the difference in the oxidation state of heme Fe, the acid–alkaline transition in metMb is similar to oxygenation of Mb in terms of the simultaneous changes in the heme Fe coordination and spin states. The oxygenation of Mb results in a change of the Fe-bound ligand from unliganded deoxy Mb to ligand-bound oxy Mb (Scheme 2), with a concomitant change in the spin state from the ferrous HS one, i.e., $S = 2$, to the ferrous LS one, i.e., $S = 0$.

Mb(Meso), Mb(7-PF), and Mb(2,8-DPF) have also been subjected to detailed studies on the ligand binding properties on the basis of not only the P_{50} values determined through measurement of an oxygen equilibrium curve (OEC),^{32,33} but also the association and dissociation rate constants for O₂ ($k_{\text{on}}(\text{O}_2)$ and $k_{\text{off}}(\text{O}_2)$, respectively) and carbon monoxide (CO) ($k_{\text{on}}(\text{CO})$ and $k_{\text{off}}(\text{CO})$, respectively), obtained using the laser flash photolysis/stopped-flow technique.^{3,12,29,34,35}

We report herein the results of heme electronic structure and ligand binding studies on Mb(Meso), Mb(7-PF), and Mb(2,8-DPF) through measurements of the pK_a , P_{50} , $k_{\text{on}}(\text{O}_2)$, $k_{\text{off}}(\text{O}_2)$, $k_{\text{on}}(\text{CO})$, and $k_{\text{off}}(\text{CO})$ values. A close relationship between the pK_a value and ρ_{Fe} values of the proteins has been confirmed by the results of DFT calculations. Comparison of the pK_a and P_{50} values among the reconstituted Mbs demonstrated that the pK_a and P_{50} values of the proteins correlate well with each other, and that the former becomes smaller and the latter becomes larger with the introduction of electron-withdrawing group(s) to the heme as peripheral side chain(s).^{7–10} Kinetic analysis revealed that the decrease in the O₂ affinity (i.e., the increase in the P_{50} value) of Mb with increasing number of introduced CF₃ groups is due to the increase in the $k_{\text{off}}(\text{O}_2)$ value. In contrast, the $k_{\text{on}}(\text{CO})$ and $k_{\text{off}}(\text{CO})$ values were both almost independent of the number of introduced CF₃ groups. These findings not only unequivocally demonstrated that the O₂ affinity of Mb decreases with a decrease in the ρ_{Fe} value, but also

provided novel insights into the structure–function relationships in oxygen binding hemoproteins.

Materials and Methods

Materials and Protein Samples. All reagents and chemicals were obtained from commercial sources and used as received. Sperm whale Mb was purchased as a lyophilized powder from Biozyme and used without further purification. Mesoheme was prepared from mesoporphyrin IX dimethyl ester purchased from Aldrich. 7-PF and 2,8-DPF were synthesized as previously described.¹⁴ O₂ and CO were purchased from Sumitomo Seika Chemicals Co., Ltd. Mesoheme (Figure 1) was prepared from mesoporphyrin IX dimethyl ester purchased from Aldrich Chemical Co. The apoprotein of Mb was prepared at 4 °C according to the procedure of Teale,³⁶ and reconstitution of the apoprotein with heme was carried out by the standard procedure.³⁷ The reconstituted Mbs were concentrated to ~1 mM in an ultrafiltration cell (Amicon). The pH of each sample was measured with a Horiba F-22 pH meter equipped with a Horiba type 6069-10c electrode. The pH of the sample was adjusted using 0.2 M NaOH or HCl.

UV–Vis Absorption and NMR Spectroscopies. UV–vis absorption spectra were recorded on 10 μM protein samples in 20 mM phosphate buffer at 25 °C using a Beckman DU 640 spectrophotometer. ¹H and ¹⁹F NMR spectra were recorded on a Bruker AVANCE-400 spectrometer operating at ¹H and ¹⁹F frequencies of 400 and 376 MHz, respectively. Typical ¹H and ¹⁹F NMR spectra consisted of about 20k transients with a 100 kHz spectral width and 16k data points. The signal-to-noise ratio of the spectra was improved by apodization, which introduced 20–100 Hz line broadening. The chemical shifts of ¹H and ¹⁹F NMR spectra are given in ppm downfield from the residual ¹H²O, as an internal reference, and from trifluoroacetic acid, as an external reference, respectively.

Oxygen Equilibrium Curves. Oxygen equilibrium curves (OECs) of the proteins were measured with 30 μM protein in 100 mM phosphate buffer, pH 7.4, and 100 mM Cl[−] at 20 °C, using the previously described automatic oxygenation apparatus.³² P_{50} values were determined through nonlinear least-squares fitting of the OEC data.³³

Kinetic Measurements. Kinetic measurements of the proteins were carried out in 100 mM phosphate buffer, pH 7.40, at 20 °C using the procedure reported previously.^{3,12,29,34,35} The O₂ associations for Mb(Meso), Mb(7-PF), and Mb(2,8-DPF) were characterized through analysis of the time evolution of the absorbance at 404, 409, and 411 nm, respectively, after photolysis of their oxy forms, in the presence of various O₂ concentrations ([O₂]), using a 5 ns-pulse Nd:YAG laser (532 nm). The probe light (Xe-lamp) was passed through a monochromator before a sample with adjusting a suitable wavelength in each experiment. The fitting of the time evolution of the absorbance to the first-order rate equation yielded a pseudo-first-order rate constant for O₂ association ($k_{\text{obs}}(\text{O}_2)$), which can be expressed in terms of $k_{\text{on}}(\text{O}_2)$ and $k_{\text{off}}(\text{O}_2)$ as $k_{\text{obs}}(\text{O}_2) = k_{\text{on}}(\text{O}_2) \times [\text{O}_2] + k_{\text{off}}(\text{O}_2)$. Thus, $k_{\text{on}}(\text{O}_2)$ was obtained through analysis of the [O₂] dependence of the $k_{\text{obs}}(\text{O}_2)$ value (see Supporting Information). Pseudo-first-order rate constants for O₂ dissociation ($k_{\text{off}}(\text{O}_2)$) for Mb(Meso), Mb(7-PF), and Mb(2,8-DPF) were also measured through the analysis of the time evolution of the absorbance at 422, 425, and 423 nm, respectively, after rapidly mixing their oxy forms with excess sodium dithionite using a stopped-flow apparatus (see Supporting Information).

The CO associations for Mb(Meso), Mb(7-PF), and Mb(2,8-DPF) were similarly measured through analysis of the time evolution of the absorbance at 409, 411, and 415 nm, respectively, after the

(29) Rohlfs, R. J.; Mathews, A. J.; Carver, T. E.; Olson, J. S.; Springer, B. A.; Egeberg, K. D.; Sligar, S. G. *J. Biol. Chem.* **1990**, *265*, 3168–3176.

(30) Maxwell, J. C.; Volpe, J. A.; Barlow, C. H.; Caughey, W. S. *Biochem. Biophys. Res. Commun.* **1974**, *58*, 166–171.

(31) Tsubaki, M.; Nagai, K.; Kitagawa, T. *Biochemistry* **1980**, *19*, 379–385.

(32) Imai, K. *Methods Enzymol.* **1981**, *76*, 438–49.

(33) Imai, K. *Methods Enzymol.* **1981**, *76*, 470–86.

(34) Olson, J. S. *Method. Enzymol.* **1981**, *76*, 631–651.

(35) Matsuo, T.; Ikegami, T.; Sato, H.; Hisaeda, Y.; Hayashi, T. *J. Inorg. Biochem.* **2006**, *100*, 1265–1271.

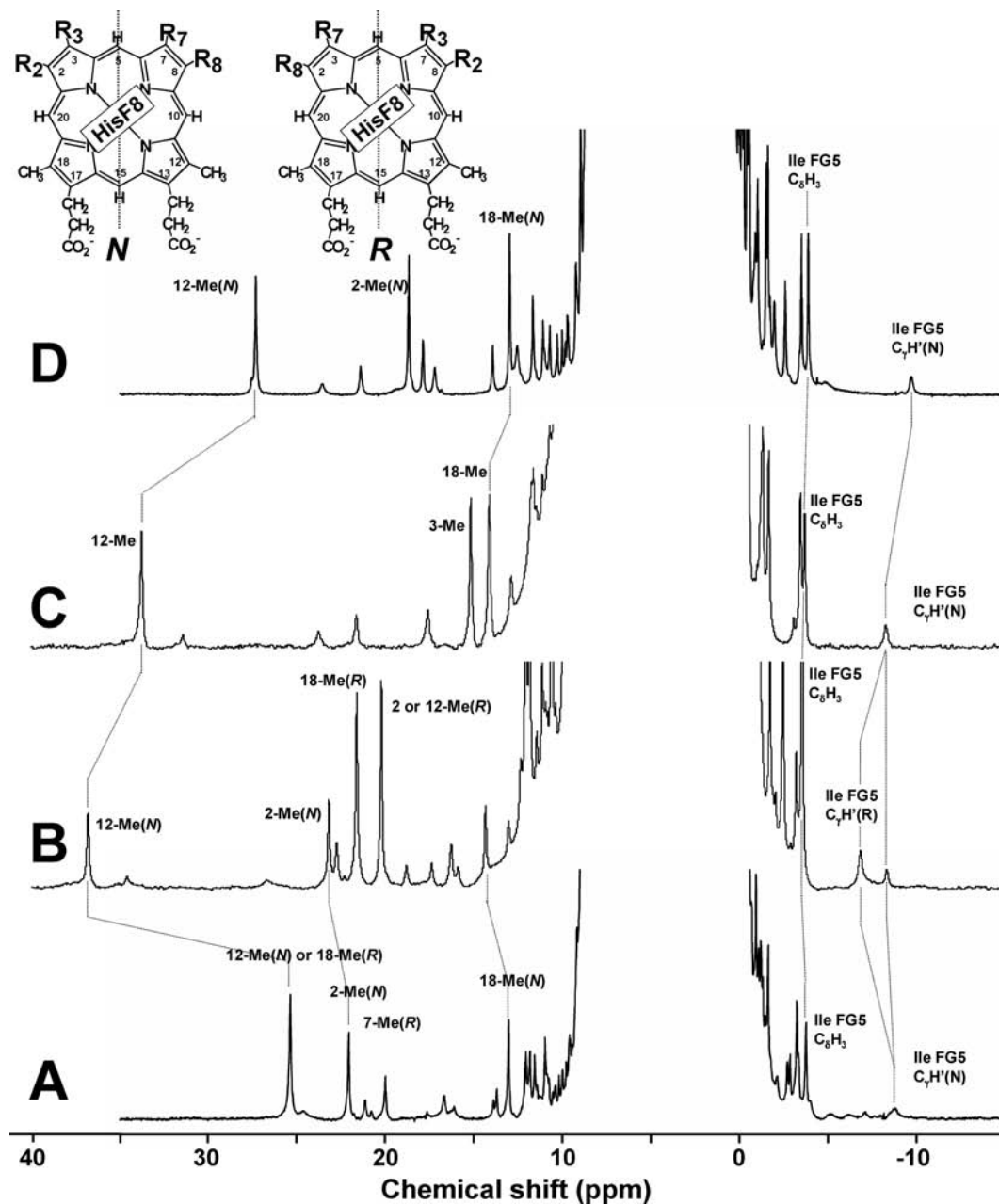
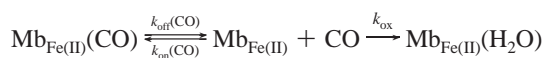


Figure 2. ^1H NMR (400 MHz) spectra of met-cyano forms of myoglobins reconstituted with mesoheme at pH 6.91 (A), 7-PF at pH 7.57 (B), 2,8-DPF at pH 7.40 (C), and native Mb at pH 7.40 (D) in 90% $\text{H}_2\text{O}/10\%$ $^2\text{H}_2\text{O}$ at 25 $^\circ\text{C}$. The assignments of heme methyl and Ile FG5^{42,43} proton signals are given with the spectra, and *N* and *R* in the inset represent the normal and reversed forms of the heme, relative to the protein.⁴⁴ Corresponding signals are connected by a broken line.

photolysis of their CO forms under 1 atm of CO, i.e., $[\text{CO}] = 9.85 \times 10^{-4}$ M. Since $k_{\text{off}}(\text{CO}) \ll k_{\text{on}}(\text{CO}) \times [\text{CO}]$, the $k_{\text{on}}(\text{CO})$ value can be determined from the pseudo-first-order rate constant for CO association ($k_{\text{obs}}(\text{CO})$) through the equation, $k_{\text{obs}}(\text{CO}) = k_{\text{on}}(\text{CO}) \times [\text{CO}]$.

The CO dissociation for the proteins was characterized utilizing the following reactions which consist of the displacement of Fe-bound CO and the oxidation of heme iron by $\text{K}_3\text{Fe}(\text{CN})_6$,^{12,35}



where $\text{Mb}_{\text{Fe(II)}}$ and $\text{Mb}_{\text{Fe(III)}}(\text{H}_2\text{O})$ represent the deoxy and met-aquo forms of the protein, respectively, and k_{ox} the rate constant for the oxidation of the heme iron. Under the experimental conditions of

high $[\text{CO}]$ and $[\text{K}_3\text{Fe}(\text{CN})_6]$, where a steady-state assumption can be made for $[\text{Mb}_{\text{Fe(II)}}]$, a pseudo-first-order rate constant for the oxidation of the proteins ($k_{\text{obs}}(\text{ox})$) can be expressed in terms of a pseudo-first-order rate constant for CO dissociation ($k_{\text{off}}(\text{CO})$), $[\text{K}_3\text{Fe}(\text{CN})_6]$, and a constant, c , as $k_{\text{obs}}(\text{ox}) = k_{\text{off}}(\text{CO}) \times [\text{K}_3\text{Fe}(\text{CN})_6] / (c + [\text{K}_3\text{Fe}(\text{CN})_6])$. The saturated value in plots of the $k_{\text{obs}}(\text{ox})$ values against $[\text{K}_3\text{Fe}(\text{CN})_6]$ affords the $k_{\text{off}}(\text{CO})$ value (see Supporting Information). The $k_{\text{obs}}(\text{ox})$ values for Mb(Meso), Mb(7-PF), and Mb(2,8-DPF) in various $[\text{K}_3\text{Fe}(\text{CN})_6]$ were determined through analysis of the time evolution of the absorbance at 531, 533, and 538 nm, respectively. The probe light (Xe-lamp) was passed through a monochromator before a sample with adjusting a suitable wavelength in each experiment. Prior to kinetic measurements, it was confirmed in preliminary experiments using a photo diode array detector that the reaction of a ligand-bound Mb with

K₃Fe(CN)₆ really yielded the corresponding met-aquo form without accumulation of any intermediates.

DFT Calculation. The DFT calculations were carried out using the Gaussian 03 program package.³⁸ Restricted spin orbital approach involving the B3LYP method, together with electron basis sets of Pople's 6-31G(d), was employed. For simplification, the calculations were performed for the 2,3,7,8,12,13,17,18-octamethylporphinatoiron(II) complex and a series of its CF₃-substituted derivatives as models for the hemes used in this study (see Supporting Information), in order to characterize the relationship between the ρ_{Fe} value and number of the CF₃ groups introduced into the porphyrin. Geometry optimization of the model compounds was carried out in the gas phase, with a fixed CH₃ or CF₃ group orientation, i.e., one C–H (or C–F) fragment was in the porphyrin plane, and the others were pointing above and below the plane (see Supporting Information). In addition, the oxidation, spin, and coordination states of the heme Fe atoms of the model compounds were assumed to be Fe(II), *S* = 0, and a 6-coordinated structure with CO ligands, respectively (see Supporting Information). Determination of the ρ_{Fe} value was carried out by well-known Mulliken charge analysis.

Results

¹H NMR Spectra of Reconstituted Mbs. ¹H NMR (400 MHz) spectra of the met-cyano forms of Mb(Meso), Mb(7-PF), and Mb(2,8-DPF) are shown in Figure 2, in comparison with that of native Mb. The paramagnetically shifted NMR signals arising from heme peripheral side chain protons and amino acid protons in close proximity to the heme in the met-cyano form of the protein have been shown to be remarkably sensitive to the heme electronic structure and the heme active site structure, respectively.^{39–41} The heme methyl proton signals of Mb(Meso), Mb(7-PF), and Mb(2,8-DPF) were observed in the shift region down to ~35 ppm, indicating that the heme Fe atoms in the proteins were in the ferric LS state. In addition, as in the case of the spectrum of native Mb, the C₇H₃ and C₈H₃ proton signals of Ile FG5 in all the reconstituted Mbs were resolved at about –4 ppm,^{42,43} demonstrating that the orientations of the hemes with respect to the polypeptide chains in these reconstituted proteins are similar to that in the native one. These results supported that the hemes of the reconstituted Mbs were accommodated properly as for that of the native protein. Finally, the observation of two sets of heme methyl proton signals in the spectra of Mb(Meso) and Mb(7-PF),²⁷ with the ratios of 1:3 and 1:2.2, respectively, is due to the presence of well-known heme orientational isomers,^{41,44} as depicted in the inset in Figure 2, and the absence of heme orientational isomers in Mb(2,8-DPF), as shown by the observation of a single set of heme methyl proton signals in the spectrum, is simply due to the C₂-symmetric molecular structure of 2,8-DPF (see Figure 1).

Acid–Alkaline Transition of metMb(2,8-DPF). We next determined the p*K*_a value for the acid–alkaline transition of metMb(2,8-DPF). The pH dependence of the absorption spectra of metMb(2,8-DPF) at 25 °C and plots of 575-nm absorption

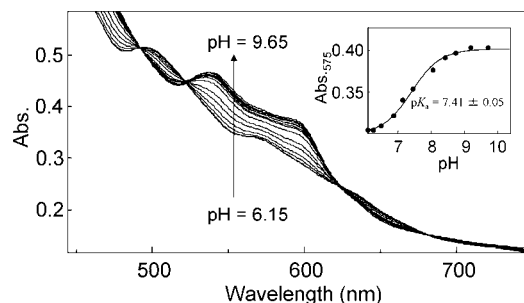


Figure 3. Absorption spectra, 445–750 nm, of metMb(2,8-DPF) at 25 °C and various pHs, 6.15–9.65, and plots of the 575-nm absorbance against pH. A p*K*_a value of 7.41 ± 0.05 was obtained.

Table 1. p*K*_a and *P*₅₀ Values of Mbs

Mb	p <i>K</i> _a ^a	<i>P</i> ₅₀ ^b (mmHg)	<i>P</i> ₅₀ ^{Plot} ^c (mmHg)	log(1/ <i>P</i> ₅₀)
Mb(Meso)	9.43 ± 0.03 ^d	0.38		0.42
Mb(7-PF)	8.57 ± 0.03 ^d	1.10		–0.041
Mb(2,8-DPF)	7.41 ± 0.05	2.80		–0.447
native Mb	8.90 ± 0.05 ^e	0.58	0.69	0.24
Mb(Deutero)	9.10 ± 0.05 ^e	0.21 ^f	0.57	0.68

^a Determined through analysis of the pH dependence of the Soret absorption band at 25 °C. ^b Determined from the oxygen equilibrium curve at pH 7.40 and 20 °C. ^c Estimated using the plots of the p*K*_a – log(1/*P*₅₀) relationship. ^d Obtained from ref 27. ^e Obtained from ref 18. ^f Obtained from ref 3.

against pH are shown in Figure 3. Quantitative fitting of the plots to the Henderson–Hasselbalch equation yielded a p*K*_a value of 7.41 ± 0.05. Since values of 9.43 ± 0.03 and 8.57 ± 0.03 have been obtained for metMb(Meso) and metMb(7-PF), respectively (Table 1),²⁷ comparison of the values among the proteins indicated that the introduction of one CF₃ group decreases the p*K*_a value by ~1 pH unit. The systematic p*K*_a decrease with increasing number of CF₃ groups could be attributed to the withdrawal of electron density from the porphyrin moiety of the heme toward these electron-attracting peripheral side chains.²⁷

O₂ Affinity. We next determined the O₂ affinities of the reconstituted Mbs by measuring OECs.^{32,33} Mb(Meso), Mb(7-PF), and Mb(2,8-DPF) exhibited *P*₅₀ values of 0.38, 1.10, and 2.80 mmHg at pH 7.40 and 20 °C, respectively (Table 1). The *P*₅₀ value increased consistently with increasing number of CF₃ substitutions, indicating that the O₂ affinity of a protein decreases with increasing electron-withdrawing power of its heme peripheral side chains, as previously reported.^{7–10} Comparison of the O₂ affinities among the proteins indicated that the introduction of one CF₃ group increases the *P*₅₀ value by a factor of ~2.8.

Kinetic Data. We finally measured the *k*_{on}(O₂), *k*_{off}(O₂), *k*_{on}(CO), and *k*_{off}(CO) values of the proteins using the laser flash photolysis/stopped-flow technique.^{3,12,29,34,35} The obtained values are summarized in Table 2. The equilibrium constants for O₂ binding (*K*(O₂)) calculated from the kinetic data, i.e., the *k*_{on}(O₂) and *k*_{off}(O₂) values, agreed well, within experimental errors, with the *P*₅₀ values of the proteins, confirming the validity of the obtained data (see Supporting Information). Comparison of the O₂ binding parameters among the proteins revealed that the *k*_{off}(O₂) value increases steadily with increasing number of CF₃ groups, whereas the *k*_{on}(O₂) value is affected little by the introduction of CF₃ groups. These results indicated that the decrease in the O₂ affinity of Mb with increasing number of CF₃ substitutions is due solely to the increase in the *k*_{off}(O₂)

(36) Teale, F. W. J. *Biochim. Biophys. Acta* **1959**, *35*, 543.

(37) La Mar, G. N.; Yamamoto, Y.; Jue, T.; Smith, K. M.; Pandey, R. K. *Biochemistry* **1985**, *24*, 3826–3831.

(38) Frisch, M. J.; et al. *Gaussian 03*, Revision E.01; Gaussian, Inc.: Wallingford, CT, 2004.

(39) La Mar, G. N.; Satterlee, J. D.; de Ropp, J. S. In *The Porphyrin Handbook*; Kadish, K., Smith, K. M., Guillard, R., Eds.; Academic Press: New York, 2000; pp 185–298.

(40) Bertini, I.; Luchinat, C. *NMR of Paramagnetic Molecules in Biological Systems*; The Benjamin/Cummings Publishing Company: Menlo Park, CA, 1986; pp 19–46.

(41) Yamamoto, Y. *Annu. Rep. NMR Spectrosc.* **1998**, *36*, 1–77.

(42) Ramaprasad, S.; Johnson, R. D.; La Mar, G. N. *J. Am. Chem. Soc.* **1984**, *106*, 5330–5335.

Table 2. O₂ and CO Binding Parameters for Mbs at pH 7.40 and 20 °C

Mb	O ₂ binding			CO binding			
	$k_{\text{on}}(\text{O}_2)$ ($\mu\text{M}^{-1} \text{s}^{-1}$)	$k_{\text{off}}(\text{O}_2)$ (s^{-1})	$K(\text{O}_2)^a$ (μM^{-1})	$k_{\text{on}}(\text{CO})$ ($\mu\text{M}^{-1} \text{s}^{-1}$)	$k_{\text{off}}(\text{CO})$ (s^{-1})	$K(\text{CO})^b$ (μM^{-1})	$K(\text{CO})/K(\text{O}_2)$
Mb(Meso)	8.2 ± 1.6	5.7 ± 1.1	1.4 ± 0.4	0.38 ± 0.07	0.048 ± 0.009	7.9 ± 2.4	5.5 ± 2.2
Mb(7-PF)	8.3 ± 1.6	17 ± 3	0.5 ± 0.1	0.32 ± 0.06	0.032 ± 0.006	10 ± 3	21 ± 8
Mb(2,8-DPF)	16 ± 3	110 ± 22	0.15 ± 0.04	0.69 ± 0.13	0.036 ± 0.007	19 ± 6	132 ± 53
Native Mb ^c	14 ± 3	12 ± 2	1.2 ± 0.3	0.51 ± 0.06	0.019 ± 0.005	27 ± 8	23 ± 9

^a Calculated from the $k_{\text{on}}(\text{O}_2)$ and $k_{\text{off}}(\text{O}_2)$ values. ^b Calculated from the $k_{\text{on}}(\text{CO})$ and $k_{\text{off}}(\text{CO})$ values. ^c Obtained from ref 29.

value with increasing number of CF₃ substitutions. Finally, in sharp contrast to the O₂ binding properties of the proteins, not only the $k_{\text{on}}(\text{CO})$ value but also the $k_{\text{off}}(\text{CO})$ one was essentially independent of the introduction of CF₃ groups as heme side chains. As a result, the CO affinities of the proteins are almost the same as each other and also comparable to that reported for native Mb.²⁹

DFT Calculations. In order to quantitatively assess the effect of the introduction of CF₃ groups as heme peripheral side chains on the ρ_{Fe} value as well as to evaluate the relationship between the ρ_{Fe} and $\text{p}K_{\text{a}}$ values, we have carried out DFT calculations for some model compounds (see Materials and Methods, and Supporting Information for details). The ρ_{Fe} value was estimated on the basis of the Mulliken charge of the heme Fe atom. The obtained Mulliken charge exhibited a stepwise increase with increasing number of introduced CF₃ groups, suggesting that the decrease in the ρ_{Fe} value is almost proportional to the number of CF₃ substitutions (Figure 4A). Although the Mulliken charges were calculated for the ferrous model compounds, a similar relationship between the ρ_{Fe} value and the number of CF₃ groups is also expected for the ferrihemes in the active sites of metMbs. In fact, as illustrated in Figure 4B, the Mulliken charges calculated for the model compounds possessing 0, 1, and 2 CF₃ groups, i.e., *bis*-CO complexes of 2,3,7,8,12,13,17,18-octamethylporphyrinato-iron(II), 2-perfluoromethyl-3,7,8,12,13,17,18-octamethylporphyrinato-iron(II), and 2,8-diperfluoromethyl-3,7,8,12,13,17,18-octamethylporphyrinato-iron(II), respectively, correlated well with the $\text{p}K_{\text{a}}$ values of metMb(Meso), metMb(7-PF), and metMb(2,8-DPF), demonstrating the remarkable sensitivity of the $\text{p}K_{\text{a}}$ value to the ρ_{Fe} value. Thus, the $\text{p}K_{\text{a}}$ value can be used as a sensitive measure for the ρ_{Fe} value.

Discussion

Effect of CF₃ Substitutions on the Electron Density of the Heme Fe Atom. Although it is readily expected, from a chemical standpoint of view, that the substitution of electron-withdrawing group(s) as heme side chain(s) decreases the porphyrin π -electron density, quantitative characterization of the influence of such substitution on the ρ_{Fe} value, particularly when the heme is located in the active site of Mb, is not an easy task. Therefore we have carried out DFT calculations for some model compounds (see Materials and Methods, and Supporting Information for details), in order to quantitatively assess the effect of the introduction of CF₃ groups as heme peripheral side chains on the ρ_{Fe} value. For simplification of the calculations, all the ethyl and propionic acid side chains of the hemes studied in this study were replaced by methyl groups in the corresponding model compounds (Figure 4A and Supporting Information). The ρ_{Fe} value was estimated on the basis of the Mulliken charge of the heme Fe atom. As illustrated in Figure 4A, the obtained Mulliken charge exhibited a small but stepwise increase with increasing number of introduced CF₃ groups, suggesting that the decrease in the ρ_{Fe} value is almost proportional to the number of CF₃ substitutions. Thus, the ρ_{Fe} value indeed decreases with

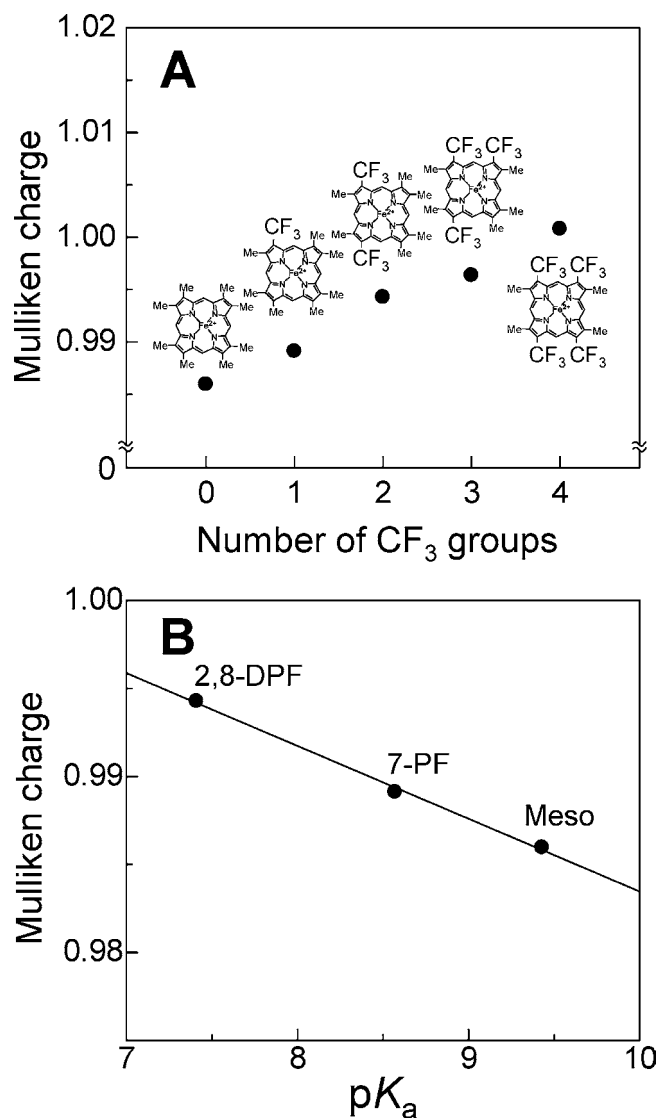


Figure 4. (A) Mulliken charges calculated for the model compounds possessing 0, 1, 2, 3, and 4 CF₃ groups as side chains, as depicted in the figure. (B) Plots of Mulliken charges of the model compounds against the $\text{p}K_{\text{a}}$ values of the proteins, with the assumption that the ρ_{Fe} values of the hemes in the proteins are reflected in the Mulliken charges calculated for the corresponding model compounds. The sizes of the error bars for the $\text{p}K_{\text{a}}$ values are larger than the diameters of the plots. The plots can be satisfactorily represented by a straight line.

the introduction of electron-withdrawing group(s) as heme side chain(s) through the electronic effect on the porphyrin π -system. A similar relationship between the ρ_{Fe} value and the number of CF₃ substitutions is also expected for hemes in the active sites of the proteins.

Correlation between the Electron Density of the Heme Fe Atom and $\text{p}K_{\text{a}}$ Values. With the assumption that the ρ_{Fe} values of the hemes in the proteins were reflected in the Mulliken

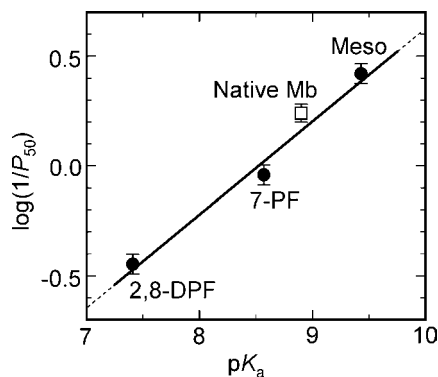


Figure 5. Plots of the pK_a values against the quantity $\log(1/P_{50})$ for Mb(Meso), Mb(7-PF), and Mb(2,8-DPF), indicated by ●. The pK_a values were determined at 25 °C, while the P_{50} values were measured at 20 °C and pH 7.40. The sizes of the error bars for the pK_a values are larger than those for the plots. The plots can be satisfactorily represented as a straight line. The pK_a value of 8.90 ± 0.03^{10} for native Mb yielded 0.16 ± 0.03 for the $\log(1/P_{50})$ value, indicated by □, i.e., a P_{50} value of 0.69 ± 0.03 mmHg, which is similar to the observed value of 0.58 mmHg at 20 °C and pH 7.40.

charges calculated for the corresponding model compounds, the Mulliken charges were plotted against the pK_a values of the proteins (Figure 4B). The plots can be satisfactorily represented by a straight line, which demonstrated that, with increasing number of introduced CF₃ groups, the Mulliken charge increases and the pK_a value decreases, respectively. As described above, the increase in the Mulliken charge with increasing number of CF₃ substitutions can be simply attributed to the decrease in the porphyrin π -electron density due to the introduction of electron-withdrawing groups. Furthermore, the decrease in the pK_a value with increasing number of the CF₃ substitutions can be also attributed to the effect of the CF₃ substitutions on the electronic properties of the Fe-bound OH⁻ in the alkaline form. The backward reaction of the acid–alkaline transition (Scheme 1) can be considered as protonation of the Fe-bound OH⁻. Since the introduction of electron-withdrawing CF₃ groups as heme side chains results in removal of an electron from the Fe-bound OH⁻ as well as the heme Fe atom, the proton affinity of the Fe-bound OH⁻ is thought to decrease with increasing number of CF₃ substitutions, which leads to a decrease in the pK_a value. The correlation between the Mulliken charges calculated for the model compounds and the pK_a values of the reconstituted Mbs (Figure 4B) supported that the ρ_{Fe} value is indeed reflected in the pK_a value. Although the pK_a value of metMb has been shown to be affected by interaction between the heme and the polypeptide chain in the active site of the protein, in addition to the ρ_{Fe} value,²⁷ the linear plots in Figure 4B suggest that the heme–protein interactions in the present proteins are similar to each other.

Correlation between the O₂ Affinity ($1/P_{50}$) and pK_a Values. We finally examined the correlation between the O₂ affinity ($1/P_{50}$) and pK_a values of the proteins. Considering that the reactivity of the heme Fe atom is regulated by its electronic nature, it is likely that the oxygen affinity, and hence the $1/P_{50}$ value, of Mb is affected by the ρ_{Fe} value. Therefore the $1/P_{50}$ and pK_a values can be related to each other through the ρ_{Fe} value. In fact, the pK_a value correlated well with the quantity $\log(1/P_{50})$ in such a manner that the $1/P_{50}$ value increased by a factor of 2.7 with an increase of 1 pK_a unit (Figure 5). Assuming a linear relationship between pK_a and $\log(1/P_{50})$ ($pK_a - \log(1/P_{50})$ relationship), the P_{50} values of Mbs could be estimated from their pK_a values. For example, in the case of metMb(7-

PF), the protein exists as a mixture of two heme orientational isomers,⁴⁴ i.e., the *N* and *R* forms (see the inset in Figure 2), in a ratio of 1: 2.2, the *N* and *R* forms exhibiting pK_a values of 8.32 ± 0.03 and 8.62 ± 0.03 , respectively.²⁷ Based on the linear $pK_a - \log(1/P_{50})$ relationship, P_{50} values of 1.22 ± 0.04 and 0.91 ± 0.03 mmHg were estimated for the *N* and *R* forms, respectively, from their pK_a values. Furthermore, a value of 0.69 ± 0.03 mmHg at 20 °C was estimated for the native metMb from its pK_a value of 8.90 ± 0.05^{18} at 25 °C. The estimated value was similar to the 0.58 mmHg observed at 20 °C and pH 7.40 (Table 1). On the other hand, the P_{50} value of 0.57 ± 0.03 mmHg estimated from the pK_a value of 9.10 ± 0.05^{18} for metMb reconstituted with deuteroheme (see structure in Figure 1) (metMb(Deutero)) was considerably larger than the observed value of 0.21 mmHg.³ The disagreement between the estimated and observed P_{50} values for this protein suggested that the heme–protein interaction in Mb(Deutero) is different from those in the other Mbs characterized in this study, possibly due to the differences in the sizes of the peripheral side chains at positions 3 and 8 (Figure 1), as manifested in its larger $k_{on}(O_2)$ value.¹⁰ Consequently, the linear $pK_a - \log(1/P_{50})$ relationship in Figure 5 appeared to be applicable to Mbs in which heme–protein interactions are similar to that in native Mb.

Mechanism Underlying the Effect of the Electron Density of the Heme Fe Atom on the O₂ Affinity of Mb. The mechanism underlying the effect of the electron density of the heme Fe atom on the O₂ affinity of Mb is clearly manifested in the kinetic data in Table 2. The $k_{off}(O_2)_{calc}$ value steadily increased with increasing number of introduced CF₃ groups, whereas the $k_{on}(O_2)$ value was affected little by the CF₃ substitutions, demonstrating the remarkably high sensitivity of the $k_{off}(O_2)$ value to the ρ_{Fe} value. These results demonstrated that the decrease in the O₂ affinity of Mb upon the introduction of electron-withdrawing CF₃ groups is due to the increase in the $k_{off}(O_2)$ value. An Fe³⁺–O₂⁻-like species has been expected for the Fe²⁺–O₂ bond in the oxy form of the protein (Scheme 2),^{30,31} and hence the withdrawal of electron density from the porphyrin moiety of the heme toward the electron-attracting peripheral side chains is thought to hinder the formation of this Fe³⁺–O₂⁻-like species through obstruction of Fe–O bond polarization. Since O₂ dissociation from the heme Fe atom is thought to occur only at the Fe²⁺–O₂ bond, the stabilization of the Fe²⁺–O₂ bond over the Fe³⁺–O₂⁻-like one with increasing number of electron-withdrawing CF₃ groups should result in an increase in the $k_{off}(O_2)$ value. In addition, the increase in the $k_{off}(O_2)$ value with increasing number of CF₃ substitutions can be also interpreted in terms of well-known distal hydrogen-bonding, i.e., the hydrogen-bonding between the Fe-bound O₂ and distal His (His E7)⁴⁵ (Scheme 2). In oxy Mb, the binding of O₂ to the heme iron has been shown to be stabilized significantly by distal hydrogen-bonding.^{5,29} The distal hydrogen-bonding is expected to be strengthened in the Fe³⁺–O₂⁻-like species relative to that in the Fe²⁺–O₂ one, due to the difference in the partial negative charge on the bound ligand. Consequently, the increase in the $k_{off}(O_2)$ value upon the CF₃ substitutions can be attributed to the weakening of the distal hydrogen-bonding as a result of stabilization of the Fe²⁺–O₂ species over the Fe³⁺–O₂⁻-like one. These mechanisms are supported by the kinetic data for the CO binding to Mb, which demonstrate that, in sharp contrast

(43) Emerson, S. D.; La Mar, G. N. *Biochemistry* **1990**, *29*, 1545–1556.

(44) La Mar, G. N.; Budd, D. L.; Viscio, D. B.; Smith, K. M.; Langry, L. C. *Proc. Natl. Acad. Sci. U. S. A.* **1978**, *75*, 5755–5759.

(45) Phillips, S. E.; Schoenborn, B. P. *Nature* **1981**, *5818*, 81–2.

to the case of the O₂ binding to the protein, not only the $k_{\text{on}}(\text{CO})$ value, but also the $k_{\text{off}}(\text{CO})$ one is essentially independent of the ρ_{Fe} value (Table 2). Although the electronic nature of the Fe-CO bond of the CO form of the protein is also expected to be perturbed to some extent on alteration of the ρ_{Fe} value, the present results demonstrate that such electronic perturbation of the Fe-CO bond is not sharply reflected in the kinetics of the CO binding to Mb, as was pointed out previously.⁴ Thus, the O₂ and CO binding properties of the proteins are different from each other in terms of the relation to the ρ_{Fe} value. These results further supported our conclusion that the O₂ affinity of the protein is regulated by the electronic properties of heme peripheral side chains through their effects on the $k_{\text{off}}(\text{O}_2)$ value. This finding not only resolves the long-standing issue of the relationship between the O₂ affinity of Mb and the electronic properties of heme peripheral side chains but also provides new insights into the structure–function relationship of the protein.

Molecular Mechanism Responsible for Discrimination between O₂ and CO. We finally discuss the effects of the introduction of electron-withdrawing CF₃ group(s) to the heme as peripheral side chain(s) on the ligand discrimination between O₂ versus CO. As described above, the O₂ and CO affinities of the protein were found to be affected quite differently by the CF₃ substitutions, i.e., the former decreases steadily with increasing number of substitutions, whereas the latter is affected little. As a result, the introduction of electron-withdrawing group(s) enhances preferential binding of CO to the protein over O₂, i.e., the $K(\text{CO})/K(\text{O}_2)$ value increases with increasing number of CF₃ substitution (Table 2). Thus, changes in the electron-withdrawing ability of heme peripheral side chains can preferentially inhibit or enhance O₂ binding relative to CO binding. This finding provides new insights into how heme peripheral side chains regulate the ligand discrimination of the protein.

Conclusion

In summary, using the $\text{p}K_{\text{a}}$ value as a sensitive and quantitative measure of the effect of heme peripheral side chain modification on the electron density of the heme Fe atom, we have confirmed that the introduction of electron-withdrawing group(s) to the heme as peripheral side chain(s) leads to a decrease in the electron density of the heme Fe atom, which in turn decreases the O₂ binding affinity of Mb.^{7–9} Kinetic studies

on reconstituted Mbs possessing various numbers of CF₃ groups as heme side chains revealed that the decrease in the O₂ affinity of Mb upon the introduction of CF₃ substitutions is due solely to an increase in the $k_{\text{off}}(\text{O}_2)$ value. A Fe³⁺–O₂[–]-like species is expected for the Fe²⁺–O₂ bond in the oxy form of the protein,^{30,31} and the formation of this Fe³⁺–O₂[–]-like species is hindered by the prevention of further polarization of the Fe–O bond due to the withdrawal of electron density from the heme Fe atom toward the electron-attracting heme peripheral side chains. Consequently, the increase in the $k_{\text{off}}(\text{O}_2)$ value with increasing number of CF₃ substitutions was attributed to the stabilization of the Fe²⁺–O₂ bond over the Fe³⁺–O₂[–]-like one upon the introduction of the electron-withdrawing groups as heme side chains. Furthermore, since distal hydrogen-bonding, which stabilizes the binding of O₂ to the heme iron, is thought to be stronger in a Fe³⁺–O₂[–]-like species than in a Fe²⁺–O₂ one, the stabilization of the latter species over the former one upon CF₃ substitutions also contributes to the increase in the $k_{\text{off}}(\text{O}_2)$ value. In addition, we demonstrated that the linear $\text{p}K_{\text{a}} - \log(1/P_{50})$ relationship is useful for analyzing the tuning of intrinsic heme Fe reactivity through the electronic properties of heme peripheral side chains. Finally, we found that the O₂ affinity of the protein decreases steadily with increasing number of CF₃ substitutions, whereas the CO one is affected little. As a result, the introduction of electron-withdrawing group(s) enhances the preferential binding of CO to the protein over O₂. Thus, the electronic properties of heme peripheral side chains were found to play a crucial role in ligand discrimination.

Acknowledgment. We are indebted Prof. Takashi Hayashi (Osaka University) for valuable discussion and to Mr. Kazuya Mizuseki for assistance with the preliminary NMR experiments. This work was supported by a Grant-in-Aid for Scientific Research on Innovative Areas (No. 21108505, “ π -Space”) from the Ministry of Education, Culture, Sports, Science and Technology, Japan, the Yazaki Memorial Foundation for Science and Technology, and the NOVARTIS Foundation (Japan) for the Promotion of Science.

Supporting Information Available: Additional figures and complete ref 38. This material is available free of charge via the Internet at <http://pubs.acs.org>.

JA909891Q